Combination of ferromagnetic and antiferromagnetic features in Heisenberg ferrimagnets

1998 J. Phys.: Condens. Matter 10 11033

(http://iopscience.iop.org/0953-8984/10/48/023)

J. Phys.: Condens. Matter **10** (1998) 11033–11048. Printed in the UK PII: S0953-8984(98)96865-5

Combination of ferromagnetic and antiferromagnetic features in Heisenberg ferrimagnets

Shoji Yamamoto†, Takahiro Fukui‡, Klaus Maisinger§ and Ulrich Schollwöck§

† Department of Physics, Faculty of Science, Okayama University, Tsushima, Okayama 700-8530, Japan

‡ Institut für Theoretische Physik, Universität zu Köln, Zülpicher Strasse 77, 50937 Köln, Germany

§ Sektion Physik, Ludwig-Maximilians-Universität München, Theresienstrasse 37, 80333 Munich, Germany

Received 18 August 1998

Abstract. We investigate the thermodynamic properties of Heisenberg ferrimagnetic mixed-spin chains both numerically and analytically with particular emphasis on the combination of ferromagnetic and antiferromagnetic features. Employing a new density-matrix renormalization-group technique as well as a quantum Monte Carlo method, we reveal the overall thermal behaviour: at very low temperatures, the specific heat and the magnetic susceptibility multiplied by the temperature behave like $T^{1/2}$ and T^{-1}, respectively, whereas at intermediate temperatures, they exhibit a Schottky-like peak and a minimum, respectively. Developing the modified spin-wave theory, we complement the numerical findings and give precise estimates for the low-temperature behaviour.

1. Introduction

Low-dimensional quantum magnets with two kinds of antiferromagnetically exchange-coupled centre have been attracting much interest recently. Several authors [1–4] constructed integrable Hamiltonians and extracted suggestive critical phenomena from them. Alternating-spin antiferromagnets with singlet ground states have stimulated us to study the nontrivial gap problem again [5]. Employing the nonlinear-σ-model technique, various mixed-spin systems such as linear chains [6, 7] and ladders [8] have been systematically studied with particular emphasis on the competition between massive and massless phases.

In this area, a remarkable level of attention has quite recently been directed towards ferrimagnetic mixed-spin chains [9–19], which are the subject of the present article. In fact, pioneering attempts [20] to study Heisenberg ferrimagnets had already been made experimentally in the 1980s in conjunction with theoretical investigations. Kahn *et al* [21] made extensive chemical explorations into the families of compounds $ACu(pba)(H_2O)_3{\cdot}nH_2O$ and $ACu(pbaOH)(H_2O)_3{\cdot}nH_2O$, where A = Mn, Fe, Co, Ni, Zn, pba = 1, 3-propylenebis(oxamato), and pbaOH = 2-hydroxy-1, 3-propylenebis(oxamato). However, the ferrimagnetism itself may not have been their main focus of interest; but they took great interest in the design of a molecule-based ferromagnet. While Drillon *et al* [22] performed a systematic exact-diagonalization study of mixed-spin chains, the chain lengths that they treated were not large enough to provide a basis for discussing

0953-8984/98/4811033+16$19.50

the universal quantum ferrimagnetic behaviour, especially at low temperatures. The recent renewal of interest in ferrimagnetic spin chains has led to a second wave of explorations—not only in the theoretical field [9–19] but also in the experimental one [23, 24]. Hagiwara *et al* have performed susceptibility measurements on a bimetallic chain compound, $NiCu(pba)(D_2O)_3{\cdot}2D_2O$, and succeeded in obtaining fundamental parameters of the sample. In an attempt to make a significant advance towards solving this challenging problem and in order to further stimulate experimental interest, we give here an extensive argument regarding the thermal behaviour of Heisenberg ferrimagnetic spin chains.

Since we may expect gapless excitations from magnetic ground states, we are less interested in whether the system is massless or massive. Using a field-theoretical argument, Alcaraz and Malvezzi [9] predicted that mixed-spin isotropic Heisenberg ferrimagnets should exhibit quadratic dispersion relations. Their prediction was numerically verified, and the quadratic dispersion was explicitly illustrated [14]. Thus, quantum ferrimagnets are expected to behave like ferromagnets at low temperatures. On the other hand, conventional spin-wave calculations [10, 12] and a perturbation approach [14] with respect to bond alternation suggest that quantum ferrimagnets should exhibit nontrivial gapped excitations as well, which have the effect of enhancing the ground-state magnetization and are therefore of antiferromagnetic nature. A quantum Monte Carlo (QMC) technique and an exact-diagonalization method [14] actually indicated two distinct low-lying excitations and showed that the mixed nature remains unchanged as long as the model is isotropic.

Motivated by the revealed low-energy structure, two of the present authors [17] investigated the thermodynamic properties of Heisenberg ferrimagnetic spin chains, focusing on the idea of coexisting ferromagnetic and antiferromagnetic aspects. Although they introduced a modified spin-wave (MSW) theory as well as a QMC method, the quantitative description of thermal quantities given was not successful, especially at low temperatures. In order to enquire further into the low-temperature behaviour, we employ here additional numerical tools. A quantum transfer-matrix (QTM) method allows us to observe how the ferromagnetic character increases in dominance with the increase of the system size. A brand-new density-matrix renormalization-group (DMRG) technique helps us to extend the investigation into the low-temperature region, which has never been achieved before. Furthermore, taking account certain interactions between spin waves, we refine the MSW theory so as to produce a more accurate description of the thermal quantities at low temperatures. Although it is rather hard, even with interacting spin waves, to obtain a quantitative description of the overall thermal behaviour, a grand-canonical approach to ferrimagnets in terms of spin waves is suggestive, and is interesting in itself. We give a full argument regarding how the conventional spin-wave theory should be *modified* when attempting to construct the thermodynamics of quantum ferrimagnets.

We consider two kinds of spin, S and s, alternating on a ring with antiferromagnetic exchange coupling between nearest neighbours, as described by the Hamiltonian

$$\mathcal{H} = J\sum_{j=1}^{N}(\boldsymbol{S}_j \cdot \boldsymbol{s}_j + \delta \boldsymbol{s}_j \cdot \boldsymbol{S}_{j+1}) - g\mu_{\mathrm{B}}H\sum_{j=1}^{N}(S_j^z + s_j^z) \tag{1}$$

where N denotes the number of unit cells, δ represents a bond alternation, μ_{B} is the Bohr magneton, and we have set the g-factors of spins $\boldsymbol{S}$ and $\boldsymbol{s}$ both equal to g. We assume that $S > s$, which remains general enough for describing alternating-spin ferrimagnets. The Lieb–Mattis theorem [25] shows that the Hamiltonian (1), unless a field is applied, has $[2(S-s)N+1]$-fold degenerate ground states. The ferromagnetic and the antiferromagnetic excitations, which lie in the subspaces $M < (S-s)N$ and $M > (S-s)N$, respectively, do

indeed show a quadratic dispersion and a gapped spectrum [14], where

$$M = \sum_{j=1}^{N} (S_j^z + s_j^z)$$

is the total magnetization. The antiferromagnetic gap—that is, the gap between the ground state and the lowest excitation to $M = (S - s)N + 1$—was estimated to be 1.759 14(1) J in the thermodynamic limit. The correlation length of the system is so small that it is barely as long as the unit cell [10, 12] even at the Heisenberg point $\delta = 1$.

2. Numerical study

In this section, using several numerical tools, we calculate the specific heat and the magnetic susceptibility at zero field. The spin-wave [10, 12] and the perturbation [14] calculations suggest that the low-temperature properties of the model are qualitatively the same regardless of the values of S and s as long as they differ from each other. Alcaraz and Malvezzi [9] performed finite-size calculations combined with a scaling analysis in the cases of $(S, s) = (1, 1/2)$ and $(S, s) = (3/2, 1/2)$ and indeed concluded that quadratic dispersion relations should be expected for arbitrary isotropic mixed-spin chains showing ferrimagnetism instead of antiferromagnetism. Thus we restrict our numerical investigations to the case of $(S, s) = (1, 1/2)$.

2.1. Procedure

We employ the QMC method based on the Suzuki–Trotter decomposition [26] of the chequerboard type [27]. The partition function $Z = \mathrm{Tr}[\mathrm{e}^{-\beta\mathcal{H}}]$ is approximately decomposed as

$$Z \simeq \left[\left(\prod_{i=1,3,\ldots} \mathrm{e}^{-\beta h_i/n} \prod_{i=2,4,\ldots} \mathrm{e}^{-\beta h_i/n} \right)^n \right] \tag{2}$$

where n is a Trotter number, $\beta = (k_\mathrm{B}T)^{-1}$ with the Boltzmann constant k_B, and

$$\begin{aligned} h_{2j-1} &= J\boldsymbol{S}_j \cdot \boldsymbol{s}_j - \frac{1}{2} g\mu_\mathrm{B} H(S_j^z + s_j^z) \\ h_{2j} &= J\delta \boldsymbol{s}_j \cdot \boldsymbol{S}_{j+1} - \frac{1}{2} g\mu_\mathrm{B} H(s_j^z + S_{j+1}^z). \end{aligned} \tag{3}$$

In order to accelerate the thermodynamic calculation and refine its accuracy, we make use of the improved algorithm given in reference [28]. Calculations are carried out at several values of n and N, and they are extrapolated to the limits $n \to \infty$ and $N \to \infty$. Although we have treated chains of $N = 24$, $N = 32$, and $N = 48$, the size dependence of the thermal quantities is so weak that we find no difference beyond the numerical uncertainty even between the calculations at $N = 24$ and those at $N = 32$ except for very low temperatures. Both the specific heat C and the magnetic susceptibility χ are directly evaluated [29] in a QMC sampling.

If we replace the trace by an importance sampling, it is hardly feasible to take grand-canonical averages at very low temperatures. In an attempt to avoid this difficulty, we may integrate out [30, 31] the $(1 + 1)$-dimensional Ising system, but then we have to give up either low temperatures or long chains. We can in principle reach an arbitrary low temperature at the expense of an increase in the system size and such an attempt is to a certain extent fruitful for the present system whose correlation length is very small. In fact,

constructing transfer matrices in the chain direction, we will later show QTM calculations of the specific heat. Although the QTM calculations themselves are so accurate that they can be regarded as exact, differentiating them numerically may introduce errors. Here we directly calculate the internal energy, rather than the partition function, and differentiate it numerically once. We keep the final results highly accurate by taking raw data at regular intervals of $k_{\mathrm{B}}T/J = 0.01$.

On the other hand, constructing transfer matrices in the Trotter direction, we can partly reveal the thermal behaviour of an infinite chain [32]. However, the exponential growth of the matrix size with the increase of n makes access to low temperatures unfeasible. In order to overcome this difficulty, we introduce the DMRG technique into our investigations. On the basis of White's original idea [33] developed at $T = 0$, we apply it to the renormalization of transfer matrices [34, 35] instead of Hamiltonians. This extension of the DMRG method has recently been applied to the thermodynamics of several low-dimensional magnets [36–38] and indeed produced plenty of results for us at very low temperatures.

The core idea of the so-called transfer-matrix DMRG method can be summarized as reaching large n by reducing the size of the transfer matrix with the use of the DMRG algorithm. We introduce a step width β_0 and extend the investigation successively down to lower temperatures $\beta^{-1} = (n\beta_0)^{-1}$, increasing n linearly. In order to avoid the exponential growth of the matrix size, we keep the number of states in the density matrix constant at a predetermined number m throughout the calculation. Obviously the two controllable parameters β_0 and m determine the precision of the transfer-matrix DMRG calculation. The Trotter decomposition is refined as $\beta_0 \to 0$, whereas the loss of information is reduced as $m \to \infty$. At high temperatures, we are compelled to work with small Trotter numbers, while few states are discarded. At low temperatures, the Trotter numbers are large enough, whereas many states are lost due to the large number of iterations. Thus, the convergence of the calculation predominantly depends on β_0 at high temperatures, while it depends on m at low temperatures, as was actually observed [38]. As we have conclusive QMC results at high and intermediate temperatures, we are particularly interested in low-temperature findings from the transfer-matrix DMRG calculation. We therefore invest our computational resources mainly in augmenting m. Setting $\beta_0 J$ and m to 0.2 and 128, respectively, we have found that at intermediate temperatures the specific heat is somewhat overestimated, whereas at low temperatures the precision almost reaches three digits. Calculations at $m = 80$, $m = 96$, and $m = 128$ fully converge at $T \gtrsim 0.05$, and almost converge at $0.04 \lesssim T \lesssim 0.05$. We were not able to extend the investigation to lower temperatures successfully. This is mainly due to the macroscopically degenerate ground states of ferrimagnets, for which a huge number of states must be retained in our access to the $T \to 0$ limit.

2.2. Results

We show in figure 1 the temperature dependence of the specific heat of the $(S, s) = (1, 1/2)$ Heisenberg ferrimagnetic spin chain. We find in figure 1(a) a good agreement between the QMC and DMRG calculations. At intermediate temperatures, the specific heat exhibits a Schottky-like anomaly typical of antiferromagnets. Let us consider the model at $\delta = 0$ in an attempt to clarify the origin of this characteristic peak. Now the model is decoupled into dimers and the specific heat per unit cell is simply obtained from an isolated dimer, which is a pure two-level system with doubly degenerate ground states and fourfold-degenerate excited states separated above by an energy gap $\Delta = 3J/2$. The specific heat is given by

$$\frac{C}{Nk_{\mathrm{B}}} = \frac{r(\beta\Delta)^2 \mathrm{e}^{\beta\Delta}}{(\mathrm{e}^{\beta\Delta} + r)^2} \tag{4}$$

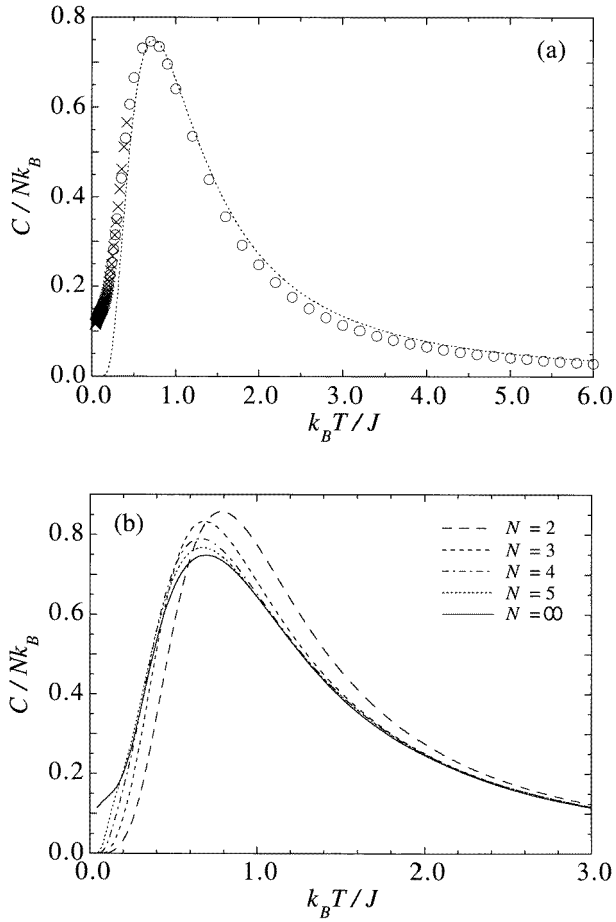

Figure 1. The temperature dependence of the specific heat per unit cell: (a) QMC findings (◯) and DMRG results (×) for $N \to \infty$. The dotted line represents the Schottky-type specific heat (2.9). The numerical uncertainty is smaller than the symbol size. (b) QTM calculations for various values of N, where we show the $N \to \infty$ curve as well, which is obtained by interconnecting the QMC findings for $k_BT/J \geqslant 0.4$ and the DMRG results for $k_BT/J \leqslant 0.4$.

where r is the ratio of the degeneracy of the excited states to that of the ground states. Moving away from the decoupled-dimer point, the low-lying states begin to exhibit dispersion and macroscopic degeneracy. At the Heisenberg point $\delta = 1$, for N elementary cells, the ground state is $(N + 1)$-fold degenerate, whereas the lowest antiferromagnetic excited state is $(N + 3)$-fold degenerate [25]. We note that the isolated dimer may be regarded as the Heisenberg chain with $N = 1$. Now we make an attempt to fit the intermediate-temperature behaviour to the curve (4), allowing only a single additional adjustable parameter A:

$$\frac{C}{Nk_B} = \frac{Ar(\beta\Delta)^2 e^{\beta\Delta}}{(e^{\beta\Delta} + r)^2}. \tag{5}$$

Here we replace r and Δ by their values at the Heisenberg point, the degeneracy ratio of the lowest antiferromagnetic excited states to the ground states and the gap between them,

respectively:

$$r = \lim_{N\to\infty} \frac{N+3}{N+1} = 1 \qquad \Delta = 1.759\,J. \tag{6}$$

We obtain a good fit with $A = 1.7$, which is also shown in figure 1(a). We stress that the Schottky-type specific heat (5) not only fits the peak but also describes well the high-temperature decay. Equation (5) combined with the condition (6) gives an asymptotic high-temperature behaviour $1.3(\beta J)^2$, which agrees well with the high-temperature series-expansion result $(\beta J)^2$ [17]. Thus we find that the temperature dependence of the specific heat straightforwardly reflects the antiferromagnetic gap, and therefore the model can be treated well as a two-level system unless it is at low enough temperatures $k_{\mathrm{B}}T \ll \Delta \simeq 1.759\,J$.

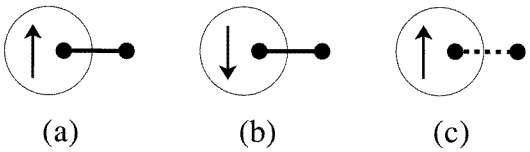

Figure 2. Schematic representations of the $M = N/2$ ground state of the $N = 1$ isolated dimer composed of spin 1 and spin 1/2 and its ferromagnetic (b) and antiferromagnetic (c) excitations. The arrow (the bullet symbol) denotes a spin 1/2 with its fixed (unfixed) projection value. The solid (broken) segment is a singlet (triplet) pair. The circle represents an operation of constructing a spin 1 by symmetrizing the two $s = 1/2$ spins inside.

On the other hand, the DMRG results fully allow us to guess the asymptotic $T^{1/2}$-behaviour characteristic of ferromagnets. This ferromagnetic feature becomes more pronounced as we move toward the Heisenberg point from the decoupled-dimer limit or alternatively as the system size increases. With this in mind, we observe the chain-length dependence of the specific heat in figure 1(b). The naive QTM method is quite useful for short chains at low temperatures. We find that the antiferromagnetic feature is fairly well established even in short chains, whereas the increase in ferromagnetism is relatively slow. The elementary excitations of ferromagnetic nature are predominantly related to $s = 1$ spins, while those of antiferromagnetic nature originate from interactions between the two kinds of spin [14]. These excitations may be identified with the local ones within a unit cell in the vicinity of the decoupled-dimer limit, as shown in figure 2. Figure 1(b) suggests that the delocalization effect is more essential to the appearance of the ferromagnetic feature. In fact, the ferromagnetic excitations constitute a wider band than the antiferromagnetic ones [14].

We show in figure 3 the temperature dependence of the magnetic susceptibility multiplied by temperature for the $(S, s) = (1, 1/2)$ Heisenberg ferrimagnetic spin chain. We find again that the QMC and DMRG calculations are in excellent agreement. The product χT diverges as T^{-1} at low temperatures, while it approaches $[S(S+1) + s(s+1)]/3 = 11/12$ at high temperatures. The low-temperature divergence is reminiscent of the ferromagnetic susceptibility [41]. We further note that χT shows a minimum at the shift from the quantum ferromagnetic behaviour to the classical paramagnetic behaviour. Generally χT is a monotonically decreasing function for ferromagnets, while it is a monotonically increasing function for antiferromagnets [39]. The susceptibilities of gapped antiferromagnets such as Haldane systems vanish exponentially [28, 29, 40]. Hence the temperature dependence that we are observing may be regarded as a ferromagnetic-to-antiferromagnetic crossover. In

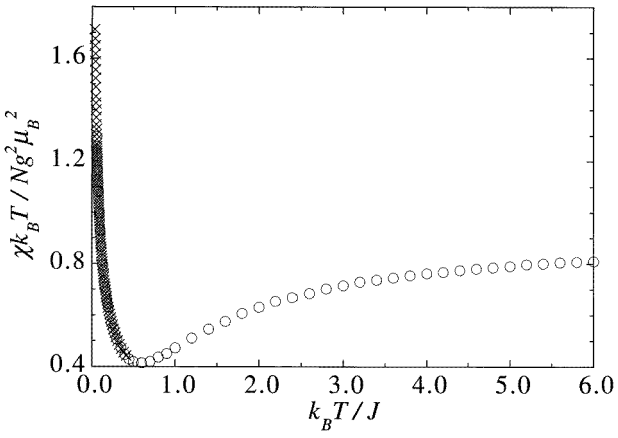

Figure 3. The temperature dependence of the magnetic susceptibility multiplied by the temperature per unit cell: QMC findings (◯) and DMRG results (×) for $N \to \infty$. The numerical uncertainty is smaller than the symbol size.

fact, the minimum of χT appears at a temperature around which the specific heat shows the Schottky-like peak.

To summarize, it has been demonstrated that ferrimagnets exhibit a combination of ferromagnetic and antiferromagnetic features. The DMRG technique has allowed us to have access to very low temperatures. In an attempt to extend the investigation to even lower temperatures, we develop the MSW theory for ferrimagnets [17] in the next section. We not only aim at obtaining a precise description of the low-temperature behaviour but also are interested in describing the overall thermal behaviour on the basis of the spin-wave picture.

3. The modified spin-wave approach

For years, the conventional spin-wave theory [42–44] was plagued by the difficulty that the zero-field magnetization diverges for low-dimensional magnets. The low-temperature series expansion within the theory only produces the leading term of the specific heat and nothing correct for the susceptibility. However, imposing a constraint on the magnetization, Takahashi [45, 46] succeeded in describing the low-temperature thermodynamics of low-dimensional ferromagnets. His idea was further applied to several quantum antiferromagnets [47–50] and its wide applicability was established. Recently two of the present authors [17] introduced this modified spin-wave theory into the study of quantum ferrimagnets and demonstrated that it is quite useful for understanding their characteristic features. Here we develop our argument, taking into account interactions between spin waves.

3.1. Dispersion relations

We have observed that the low-temperature thermodynamics well reflects the dispersion relation of the ferromagnetic branch, whereas the intermediate-temperature behaviour is suitably attributed to that of the gapped antiferromagnetic branch. This scenario is indeed supported by the MSW theory [17]. A combination of the ferromagnetic and antiferromagnetic spin waves on which a particular constraint is imposed reproduces the

initial $T^{1/2}$-behaviour, the Schottky-like peak, and the T^{-2}-decay of the specific heat, and the T^{-2}-divergence and the T^{-1}-decay of the susceptibility (see figure 5 and figure 6 later). However, we should recall that the conventional spin-wave calculation, based on which we started our first attempt [17] to construct the thermodynamics, considerably underestimates the antiferromagnetic gap Δ. Consequently, the MSW approach succeeds in reproducing the Schottky anomaly itself, to be sure, but fails in locating it at a correct temperature. In order to obtain a better description, we first refine the original spin-wave theory.

Let us introduce bosonic operators through the Holstein–Primakoff transformation [42]:

$$\begin{aligned} S_j^+ &= (2S - a_j^\dagger a_j)^{1/2} a_j \qquad & S_j^z &= S - a_j^\dagger a_j \\ s_j^+ &= b_j^\dagger (2s - b_j^\dagger b_j)^{1/2} & s_j^z &= -s + b_j^\dagger b_j \end{aligned} \tag{7}$$

where we regard S and s as quantities of the same order, that is, $\mathrm{O}(S) = \mathrm{O}(s)$. The Hamiltonian (1) with $\delta = 1$ and $H = 0$ is expressed in terms of the bosonic operators as

$$\mathcal{H} = E_{\mathrm{class}} + \mathcal{H}_0 + \mathcal{H}_1 + \mathrm{O}(S^{-1}) \tag{8}$$

where

$$E_{\mathrm{class}} = -2sSJN \tag{9}$$

$$\mathcal{H}_0 = J \sum_j \left\{ 2s a_j^\dagger a_j + 2S b_j^\dagger b_j + \sqrt{sS}\left[(a_j + a_{j+1}) b_j + \mathrm{HC} \right] \right\} \tag{10}$$

$$\begin{aligned} \mathcal{H}_1 = -J \sum_j \Bigg\{ & \frac{1}{4} \left[\sqrt{S/s} (a_j + a_{j+1}) b_j^\dagger b_j^2 + \sqrt{s/S} a_j^\dagger a_j^2 (b_j + b_{j-1}) + \mathrm{HC} \right] \\ & + (a_j^\dagger a_j + a_{j+1}^\dagger a_{j+1}) b_j^\dagger b_n \Bigg\}. \end{aligned} \tag{11}$$

The treatment of the quartic interaction (11) is not as canonical as that of the quadratic Hamiltonian (10). A variety of approaches are possible [18]. Here, in an attempt to obtain the dispersion relations beyond the noninteracting spin-wave theory, we first diagonalize $\mathcal{H}_0$ and next extract corrections from $\mathcal{H}_1$.

The Bogoliubov transformation

$$\begin{aligned} \alpha_k &= (\cosh\theta_k) a_k + (\sinh\theta_k) b_k^\dagger \\ \beta_k &= (\sinh\theta_k) a_k^\dagger + (\cosh\theta_k) b_k \end{aligned} \tag{12}$$

combined with

$$\begin{aligned} a_k &= \frac{1}{\sqrt{N}} \sum_j \mathrm{e}^{\mathrm{i}k(j-1/4)} a_j \\ b_k &= \frac{1}{\sqrt{N}} \sum_j \mathrm{e}^{-\mathrm{i}k(j+1/4)} b_j \end{aligned} \tag{13}$$

and

$$\tanh 2\theta_k = -\frac{2\sqrt{Ss}}{S+s} \cos\left(\frac{k}{2}\right) \tag{14}$$

diagonalizes $\mathcal{H}_0$ as [10, 12]

$$\mathcal{H}_0 = E_0 + J \sum_k (\omega_k^- \alpha_k^\dagger \alpha_k + \omega_k^+ \beta_k^\dagger \beta_k) \tag{15}$$

where we have taken twice the lattice constant as unity. The first term in (15) is the $O(S^1)$ quantum correction to the ground-state energy,

$$E_0 = J\sum_k[\omega_k - (S+s)] \tag{16}$$

with

$$\omega_k = \sqrt{(S-s)^2 + 4Ss\sin^2(k/2)}. \tag{17}$$

The following $O(S^1)$ terms are the ferromagnetic and antiferromagnetic spin-wave modes, whose dispersion relations are, respectively, given by

$$\omega_k^{\mp} = \omega_k \mp (S-s). \tag{18}$$

The lower-energy mode shows a quadratic dispersion relation at small values of k, which is consistent with the initial $T^{1/2}$-behaviour of the specific heat. On the other hand, the gap between the two branches is exactly J, which considerably contradicts the numerical estimate of $1.759\,J$.

Now we pick up relevant contributions to the dispersions, as well as to the ground-state energy, from $\mathcal{H}_1$. Employing the Wick theorem, we rewrite $\mathcal{H}_1$ as

$$\mathcal{H}_1 = E_1 - J\sum_k(\delta\omega_k^-\alpha_k^\dagger\alpha_k + \delta\omega_k^+\beta_k^\dagger\beta_k) + \mathcal{H}_{\rm irrel} + \mathcal{H}_{\rm quart} \tag{19}$$

where $H_{\rm irrel}$ contains irrelevant terms such as $\alpha_k\beta_k$ and $\mathcal{H}_{\rm quart}$ contains residual two-body interactions, both of which are neglected in the following. The $O(S^0)$ correction to the ground-state energy, E_1, and those to the dispersions, $\delta\omega_k^{\pm}$, are, respectively, given by

$$E_1 = -2JN[\Gamma_1^2 + \Gamma_2^2 + (\sqrt{S/s} + \sqrt{s/S})\Gamma_1\Gamma_2] \tag{20}$$

$$\delta\omega_k^{\pm} = 2(S+s)\Gamma_1\frac{\sin^2(k/2)}{\omega_k} + \frac{\Gamma_2}{\sqrt{Ss}}[\omega_k \pm (S-s)] \tag{21}$$

with

$$\begin{aligned}\Gamma_1 &= \frac{1}{2N}\sum_k(\cosh 2\theta_k - 1)\\ \Gamma_2 &= \frac{1}{2N}\sum_k\cos\left(\frac{k}{2}\right)\sinh 2\theta_k.\end{aligned} \tag{22}$$

In the thermodynamic limit, the key constants Γ_1 and Γ_2 with $(S,s) = (1, 1/2)$ are estimated to be 0.304 887 and $-0.337\,779$, respectively. Up to $O(S^0)$, we end up with the Hamiltonian

$$\mathcal{H} \simeq E_{\rm g} + J\sum_k(\tilde{\omega}_k^-\alpha_k^\dagger\alpha_k + \tilde{\omega}_k^+\beta_k^\dagger\beta_k) \tag{23}$$

where

$$\tilde{\omega}_k^{\pm} = \omega_k^{\pm} - \delta\omega_k^{\pm} \tag{24}$$

$$E_{\rm g} = E_{\rm class} + E_0 + E_1. \tag{25}$$

In figure 4 we plot $\tilde{\omega}_k^{\pm}$ and $\omega_k^{\pm}$ as functions of k at $(S,s) = (1, 1/2)$ with the previous numerical estimates [14] for finite chains. We find that the antiferromagnetic mode is now improved to a great extent. Furthermore, the bandwidths of the two branches, which are exactly the same within the noninteracting spin-wave theory, are now indeed different, due to the interactions. The gap $\Delta = J$ is replaced by $\Delta = (1 - 2\Gamma_2)J \simeq 1.676\,J$, which is much closer to the exact value of $1.759\,J$. The ground-state energy $E_{\rm g}$ is also refined: $E_{\rm class} + E_0 \simeq -1.437\,J$, while $E_{\rm class} + E_0 + E_1 \simeq -1.459\,J$, where the exact value is $-1.454\,J$.

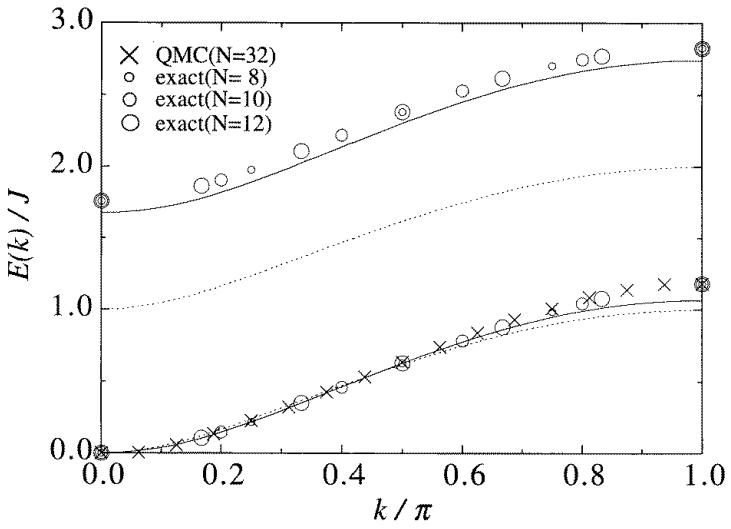

Figure 4. Dispersion relations of the lowest-energy states in the subspaces $M = N/2 \mp 1$. The noninteracting spin-wave result (dotted lines) and an improved calculation taking into account interactions between spin waves (solid lines). Previous numerical calculations [14] are also shown for the sake of comparison. Here we plot the excitation energy $E(k)$ taking the ground-state energy and twice the lattice constant as zero and unity, respectively.

3.2. Thermodynamics

Now let us start our MSW theory from the above-obtained improved dispersion relations. At finite temperatures we replace $\alpha_k^\dagger \alpha_k$ and $\beta_k^\dagger \beta_k$ in the spin-wave Hamiltonian by

$$\tilde{n}_k^\pm \equiv \sum_{n^-,n^+} n^\pm P_k(n^-, n^+)$$

where $P_k(n^-, n^+)$ is the probability of n^- ferromagnetic and n^+ antiferromagnetic spin waves appearing in the k-momentum state and satisfies

$$\sum_{n^-,n^+} P_k(n^-, n^+) = 1 \tag{26}$$

for all values of k. Then the free energy at zero field is given by

$$F = E_\mathrm{g} + \sum_k (\tilde{n}_k^- \omega_k^- + \tilde{n}_k^+ \omega_k^+) + k_\mathrm{B}T \sum_k \sum_{n^-,n^+} P_k(n^-, n^+) \ln P_k(n^-, n^+). \tag{27}$$

We now carry out the minimization of the free energy (27) with respect to the $P_k(n^-, n^+)$ under a particular constraint as well as the trivial constraint (26). The original idea introduced by Takahashi [45, 46] was that the zero-field magnetization should be zero. This constraint works quite well, especially for ferromagnets, where it serves to control the number of Holstein–Primakoff bosons. Let us apply the same constraint to the present model:

$$\langle S^z + s^z \rangle = (S - s)N - \sum_k \sum_{\sigma=\pm} \sigma \tilde{n}_k^{-\sigma} = 0 \tag{28}$$

where

$$S^z = \sum_j S_j^z \qquad \text{and} \qquad s^z = \sum_j s_j^z.$$

Equation (28) indicates that the thermal fluctuation

$$\sum_k \sum_\sigma \sigma \tilde{n}_k^{-\sigma}$$

should be constrained to take the value of the *classical* magnetization, $(S-s)N$. The free energy and the magnetic susceptibility at thermal equilibrium are then given by

$$F = E_g + \mu(S-s)N - k_B T \sum_k \sum_{\sigma=\pm} \ln(1+\tilde{n}_k^\sigma) \tag{29}$$

$$\chi = \frac{(g\mu_B)^2}{3k_B T} \sum_k \sum_{\sigma=\pm} \tilde{n}_k^\sigma (1+\tilde{n}_k^\sigma) \tag{30}$$

with

$$\tilde{n}_k^\pm = \frac{1}{e^{(J\tilde{\omega}_k^\pm \pm \mu)/k_B T} - 1} \tag{31}$$

where μ is a Lagrange multiplier due to the condition (28). The susceptibility has been obtained by calculating $\chi = (g\mu_B)^2(\langle M^2\rangle - \langle M\rangle^2)/3NT$ [45]. Equations (29) and (30) are expanded in powers of $T^{1/2}$ at low temperatures as

$$\frac{C}{Nk_B} = \frac{3}{4}\left(\frac{S-s}{Ss}\right)^{1/2} \frac{\zeta(\frac{3}{2})}{\sqrt{2\pi}} \tilde{t}^{\,1/2} - \frac{1}{Ss}\tilde{t} + \frac{15}{32(S-s)^{1/2}(Ss)^{3/2}} \left[\frac{(S^2+Ss+s^2)\zeta(\frac{5}{2})}{\sqrt{2\pi}} - \frac{4\zeta(\frac{1}{2})}{\sqrt{2\pi}}\right] \tilde{t}^{\,3/2} + O(\tilde{t}^{\,2}) \tag{32}$$

$$\frac{\chi J}{N(g\mu_B)^2} = \frac{Ss(S-s)^2}{3}\tilde{t}^{\,-2} - (Ss)^{1/2}(S-s)^{3/2}\frac{\zeta(\frac{1}{2})}{\sqrt{2\pi}}\tilde{t}^{\,-3/2} + (S-s)\left[\frac{\zeta(\frac{1}{2})}{\sqrt{2\pi}}\right]^2 \tilde{t}^{\,-1} + O(\tilde{t}^{\,-1/2}) \tag{33}$$

where $\zeta(z)$ is Riemann's zeta function and

$$\tilde{t} = k_B\tilde{T}/J = k_B T/J\gamma \qquad \text{with } \gamma = 1 - \Gamma_1(S+s)/Ss - \Gamma_2/Ss.$$

Surprisingly, the low-temperature series expansions (32) and (33) are exactly the same as the thermodynamic Bethe-*ansatz* calculations for the spin-1/2 ferromagnet [41] except for γ. Thus we recognize similarities between ferrimagnets and ferromagnets at low temperatures. We note, however, that ferrimagnets with $S = 2s$ should not strictly be identified with spin-s ferromagnets because of the scaling factor γ. With the interactions, the original temperature T is replaced by $\tilde{T}$ $(>T)$ or equivalently the original spins are reduced. Therefore, ferrimagnets with $S = 2s$ behave like spin-$\tilde{s}$ $(<s)$ ferromagnets, at least at low temperatures, which reminds us of the quantum spin reduction [12] in ferrimagnets. The spin-wave theory shows that the staggered magnetization is reduced to

$$(S+s)N - 2\tau \qquad \text{with } 2\tau = \sum_k [(S+s)/s\omega_k - 1].$$

Unfortunately, in the present model, the constraint introduced above is not useful at all at high temperatures, because it allows the number of bosons of each mode to diverge. In fact, under the condition of zero magnetization, the specific heat becomes a monotonically increasing function. Hence we propose an alternative constraint [17]. Let us consider the minimization of the free energy constraining the *staggered magnetization* to be zero:

$$\langle :S^z - s^z: \rangle = (S+s)N - (S+s)\sum_k \sum_{\sigma=\pm} \frac{\tilde{n}_k^\sigma}{\omega_k} = 0 \tag{34}$$

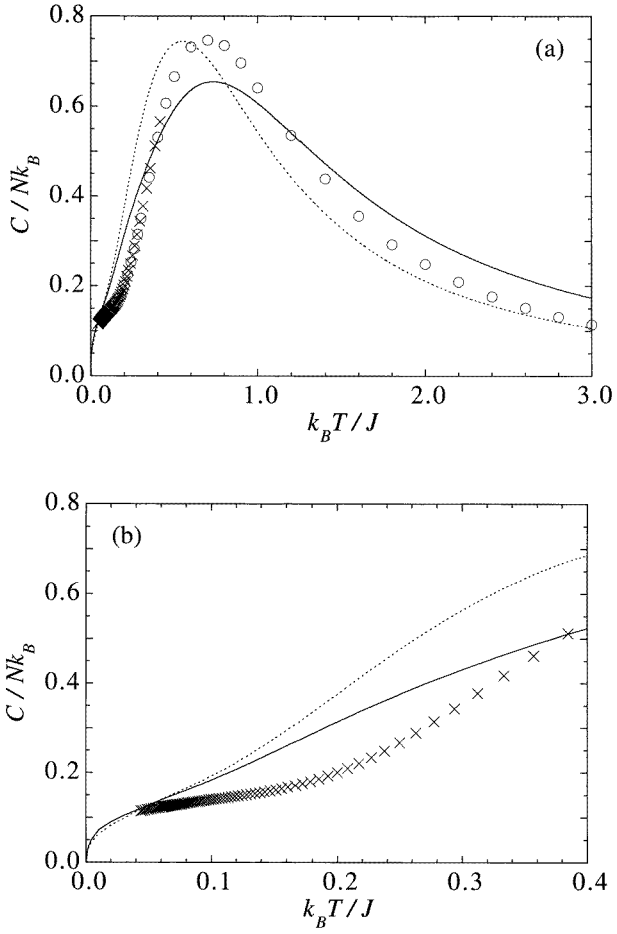

Figure 5. The temperature dependence of the specific heat per unit cell: the MSW calculation with noninteracting spin waves (dotted lines) and that with the improved dispersion relations (solid lines). The numerical findings (QMC (◯) and DMRG (×)) are also shown.

where the normal ordering is taken with respect to both operators α and β. Equation (34) implies, just as equation (28) does, that the thermal fluctuation

$$(S+s)\sum_k\sum_\sigma \tilde{n}_k^\sigma/\omega_k$$

should take the *classical* value, $(S+s)N$, rather than the renormalized value, $(S+s)N-2\tau$. We note that, on the basis of the naive idea of zero staggered magnetization without the normal ordering, we have

$$\langle S^z - s^z\rangle = (S+s)N - 2\tau - (S+s)\sum_k\sum_{\sigma=\pm}\frac{\tilde{n}_k^\sigma}{\omega_k} = 0. \tag{35}$$

Besides such a phenomenological argument, a more stringent reason drives us to adopt equation (34): condition (34) exactly reproduces the low-temperature series expansions (32) and (33), whereas condition (35) fails to do this. The conventional spin-wave theory at least leads to the correct leading term of the specific heat, which is obviously reproduced by

the MSW theory with the constraint of zero magnetization. The low-temperature behaviour must be inherent in the dispersion relation and should not be influenced by supplementary constraints. Now the set of self-consistent equations (29) and (30) is replaced by

$$F = E_{\mathrm{g}} + \mu(S+s)N - k_{\mathrm{B}}T\sum_{k}\sum_{\sigma=\pm}\ln(1+\tilde{n}_k^{\sigma}) \tag{36}$$

$$\chi = \frac{(g\mu_{\mathrm{B}})^2}{3k_{\mathrm{B}}T}\sum_{k}\sum_{\sigma=\pm}\tilde{n}_k^{\sigma}(1+\tilde{n}_k^{\sigma}) \tag{37}$$

with

$$\tilde{n}_k^{\pm} = \frac{1}{\mathrm{e}^{[J\tilde{\omega}_k^{\pm}-\mu(S+s)/\omega_k]/k_{\mathrm{B}}T}-1} \tag{38}$$

where μ is a Lagrange multiplier due to the condition (34).

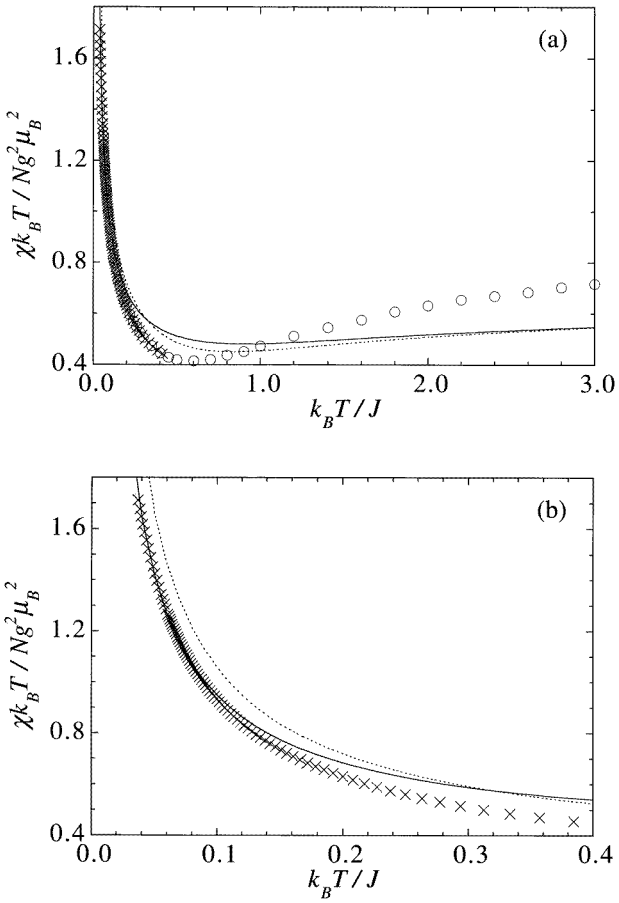

Figure 6. The temperature dependence of the magnetic susceptibility multiplied by the temperature per unit cell: the MSW calculation with noninteracting spin waves (dotted lines) and that with the improved dispersion relations (solid lines). The numerical findings (QMC (◯) and DMRG (×)) are also shown.

In the case where $(S, s) = (1, 1/2)$, we have obtained (36) and (37) numerically in the thermodynamic limit, and we illustrate them in figure 5 and figure 6, where the solid

curves represent the calculations starting from the improved dispersion relations $\tilde{\omega}_k^{\pm}$, while the dashed curves represent the calculations with $\omega_k^{\pm}$ [17] instead of $\tilde{\omega}_k^{\pm}$. Though the present calculation including the $O(S^0)$ interactions underestimates the height of the Schottky-like peak, the interactions do correct the location of the peak, which emphasizes that the gapped antiferromagnetic spin-wave mode makes the predominant contribution to this peak. We would like to attribute the unsolved discrepancy to the constraint rather than to the dispersion relations. Even though we adopt the two constraints (28) and (34) simultaneously, the results do not change significantly. This is not so surprising, because the two constraints play almost the same role at low temperatures, as the low-temperature series expansions imply, whereas only the constraint (34) is relevant at high temperatures. The precise description of the overall temperature dependence might be obtained with a temperature-dependent constraint, which is not so interesting.

We obtain the best results from the MSW theory at low temperatures. Figure 6(b) fully convinces us of the validity of the present MSW calculation. Figure 5(b) clearly reveals the low-temperature behaviour which no numerical tool has succeeded in doing. Takahashi compared his MSW findings [46] for ferromagnets with the spin-1/2 thermodynamic Bethe-*ansatz* calculations [41], and found that the MSW theory correctly describes the leading two terms of the specific heat and the leading three terms of the susceptibility in its low-temperature series expansions. We also find that the low-temperature series expansions (32) and (33) coincide with those for the spin-1/2 ferromagnet to the same extent, except for the scaling factor γ. This may be why the MSW and numerical findings for the susceptibility are closer at higher temperatures than those for the specific heat.

4. Summary

Developing an analytic argument as well as employing various numerical tools, we have investigated the thermodynamic properties of Heisenberg ferrimagnetic spin chains. Both ferromagnetic and antiferromagnetic aspects are contained in the model; they are most clearly exhibited at low and intermediate temperatures, respectively. One might say that mixed-spin chains possess mixed features. We have shown that the MSW theory, starting from the improved dispersion relations, precisely describes the low-temperature behaviour of the model. We appeal to experimentalists to carry out specific heat and susceptibility measurements of mixed-spin materials, especially at low temperatures. On the other hand, the Schottky-like peak of the specific heat and the minimum of the susceptibility–temperature product, clearly reflecting the presence of the antiferromagnetic gap, imply that the antiferromagnetic excitations are not smeared out in the ferromagnetic spectra, but stand out clearly. Hence neutron scattering measurements are also encouraged.

Acknowledgments

The authors would like to thank H-J Mikeska, S Brehmer, and S K Pati for their useful comments and fruitful discussions. This work was supported by the Japanese Ministry of Education, Science, and Culture through the Grant-in-Aid No 09740286 and by a Grant-in-Aid from the Okayama Foundation for Science and Technology. TF is supported by a JSPS Postdoctoral Fellowship for Research Abroad. Part of the numerical computation was done using the facility of the Supercomputer Centre, Institute for Solid State Physics, University of Tokyo.

References

[1] de Vega H J and Woynarovich F 1992 *J. Phys. A: Math. Gen.* **25** 4499
de Vega H J, Mezincescu L and Nepomechie R I 1994 *Phys. Rev.* B **49** 13 223
[2] Aladim S R and Martins M J 1993 *J. Phys. A: Math. Gen.* **26** L529
Martins M J 1993 *J. Phys. A: Math. Gen.* **26** 7301
[3] Fujii M, Fujimoto S and Kawakami N 1996 *J. Phys. Soc. Japan* **65** 2381
[4] Dörfel B-D and Meißner S 1997 *J. Phys. A: Math. Gen.* **30** 1831
[5] Haldane F D M 1983 *Phys. Lett.* **93A** 464
Haldane F D M 1983 *Phys. Rev. Lett.* **50** 1153
[6] Fukui T and Kawakami N 1997 *Phys. Rev.* B **55** 14 709
Fukui T and Kawakami N 1997 *Phys. Rev.* B **56** 8799
[7] Takano K 1998 *Preprint* cond-mat/9804055
[8] Fukui T and Kawakami N 1998 *Phys. Rev.* B **57** 398
Koga A, Kumada S, Kawakami N and Fukui T 1998 *J. Phys. Soc. Japan* **67** 622
[9] Alcaraz F C and Malvezzi A L 1997 *J. Phys. A: Math. Gen.* **30** 767
[10] Pati S K, Ramasesha S and Sen D 1997 *Phys. Rev.* B **55** 8894
Pati S K, Ramasesha S and Sen D 1997 *J. Phys.: Condens. Matter* **9** 8707
[11] Kolezhuk A K, Mikeska H-J and Yamamoto S 1997 *Phys. Rev.* B **55** 3336
[12] Brehmer S, Mikeska H-J and Yamamoto S 1997 *J. Phys.: Condens. Matter* **9** 3921
[13] Niggemann H, Uimin G and Zittartz J 1997 *J. Phys.: Condens. Matter* **9** 9031
Niggemann H, Uimin G and Zittartz J 1998 *J. Phys.: Condens. Matter* **10** 5217
[14] Yamamoto S 1997 *Int. J. Mod. Phys.* C **8** 609
Yamamoto S, Brehmer S and Mikeska H-J 1998 *Phys. Rev.* B **57** 13 610
[15] Ono T, Nishimura T, Katsumura M, Morita T and Sugimoto M 1997 *J. Phys. Soc. Japan* **66** 2576
[16] Kuramoto T 1998 *J. Phys. Soc. Japan* **67** 1762
[17] Yamamoto S and Fukui T 1998 *Phys. Rev.* B **57** 14 008
[18] Ivanov N B 1998 *Phys. Rev.* B **57**
Ivanov N B, Richter J and Schollwöck U 1998 *Preprint* cond-mat/9803150
[19] Maisinger K, Schollwöck U, Brehmer S, Mikeska H-J and Yamamoto S 1998 *Phys. Rev.* B **58** 5908
[20] Kahn O, Pei Y and Journaux Y 1992 *Inorganic Materials* ed D W Bruce and D O'Hare (New York: Wiley) p 95
[21] Pei Y, Verdaguer M, Kahn O, Sletten J and Renard J-P 1987 *Inorg. Chem.* **26** 138
Kahn O, Pei Y, Verdaguer M, Renard J-P and Sletten J 1988 *J. Am. Chem. Soc.* **110** 782
van Koningsbruggen P J, Kahn O, Nakatani K, Pei Y and Renard J-P 1990 *Inorg. Chem.* **29** 3325
[22] Drillon M, Gianduzzo J C and Georges R 1983 *Phys. Lett.* **96A** 413
Drillon M, Coronado E, Georges R, Gianduzzo J C and Curely J 1989 *Phys. Rev.* B **40** 10 992
[23] Hagiwara M, Minami K, Narumi Y, Tatani K and Kindo K 1998 *J. Phys. Soc. Japan* **67** 2209
[24] Fujiwara N and Hagiwara M 1998 private communication
[25] Lieb E and Mattis D 1962 *J. Math. Phys.* **3** 749
[26] Suzuki M 1976 *Prog. Theor. Phys.* **56** 1454
[27] Hirsch J E, Sugar R L, Scalapino D J and Blankenbecler R 1982 *Phys. Rev.* B **26** 5033
[28] Yamamoto S 1995 *J. Phys. Soc. Japan* **64** 4049
[29] Yamamoto S 1996 *Phys. Rev.* B **53** 3364
[30] Betsuyaku H 1984 *Phys. Rev. Lett.* **53** 629
[31] Suzuki M 1985 *Phys. Rev.* B **31** 2957
[32] Betsuyaku H 1985 *Prog. Theor. Phys.* **73** 319
Yokota T and Betsuyaku H 1986 *Prog. Theor. Phys.* **75** 46
Betsuyaku H and Yokota T 1986 *Prog. Theor. Phys.* **75** 808
[33] White S R 1992 *Phys. Rev. Lett.* **69** 2863
White S R 1993 *Phys. Rev.* B **48** 10 345
[34] Nishino T 1995 *J. Phys. Soc. Japan* **64** 3598
[35] Bursill R J, Xiang T and Gehring G A 1996 *J. Phys.: Condens. Matter* **8** L583
[36] Shibata N 1997 *J. Phys. Soc. Japan* **66** 2221
[37] Wang X and Xiang T 1997 *Phys. Rev.* B **56** 5061
[38] Maisinger K and Schollwöck U 1998 *Phys. Rev. Lett.* **81** 445
[39] Bonner J C and Fisher M E 1964 *Phys. Rev.* **135** A640
[40] Yamamoto S and Miyashita S 1993 *Phys. Rev.* B **48** 9528

[41] Takahashi M and Yamada M 1985 *J. Phys. Soc. Japan* **54** 2808
Yamada M and Takahashi M 1986 *J. Phys. Soc. Japan* **55** 2024
[42] Holstein T and Primakoff H 1940 *Phys. Rev.* **58** 1098
[43] Anderson P W 1952 *Phys. Rev.* **86** 694
[44] Kubo R 1952 *Phys. Rev.* **87** 568
[45] Takahashi M 1986 *Prog. Theor. Phys. Suppl.* **87** 233
[46] Takahashi M 1987 *Phys. Rev. Lett.* **58** 168
[47] Takahashi M 1989 *Phys. Rev.* B **40** 2494
[48] Hirsch J E and Tang S 1989 *Phys. Rev.* B **40** 4769
Tang S, Lazzouni M E and Hirsch J E 1989 *Phys. Rev.* B **40** 5000
[49] Rezende S M 1990 *Phys. Rev.* B **42** 2589
[50] Hida K 1996 *J. Phys. Soc. Japan* **65** 594